A SURVEY OF LINEAR CONTROL FOR UNICYCLE ROBOT

Dinh-Hau Vu, Thi-Ai-Van Nguyen, Vo-Minh-Dang Ly, Van-Chien Hoa, Duy-Hau Vo, Nguyen-Kha Nguyen, Minh-Linh Vo, Van-Dong-Hai Nguyen*

Ho Chi Minh city University of Technology and Education (HCMUTE)
Vo Van Ngan street, 01, Ho Chi Minh city, Vietnam

***** Corresponding author. E-mail: hainvd@hcmute.edu.vn

Abstract: Mobile robots are a subject that researchers have been developing a lot. Most of the research mainly on two-wheeled balanced robots use PID, LQR controllers, …. Currently, products such as bicycle unicycles, one wheel scooter are becoming more and more popular in many countries. In this article, our research group covers the construction of kinematic and dynamic mathematical equations, design of PID and LQR controllers using MATLAB/ Simulink.

Keywords: unicycles robot, LQR controller, PID controller, dynamic, kinematic.

1. Introduction

The unicycle was fist introduced in [1], this research has provided a mathematical equations and controllability of this model. When being first introduced [2], this model has completed design the unicycle robot based on Human Riding a Unicycle. That paper showed the mathematical equations and balance robot without controller. Therefore, this model can not be stabilized and model was still too cumbersome. But it remained a source of inspiration for later products: Honda developed UX-3 as personal vehicle and Murata Manufacturing also developed the Murata girl. In [3], a new dynamic equations are shown. This robot is devided into two parts: upper is reaction wheel pendulum and bottom is inverted pendulum which are decoupled. In this reasearch, they using the intelligent algorithm such as fuzzy for each dynamic, for high speed motion, balance time of robot become large and varying. Dynamic control for pitch and roll axes for unicycle is introduced in [4-5], they completely controlled unicycle by using robust control for roll and linear control for pitch. But, it still has a small chattering in output. Eventhough they used the signum function to reduce chattering. New type of unicycle is form with active omnidirectional wheel but this model also has the mechanical limitations [6].

To reduce the balance time for robot [3] and reduce chattering [4-5], we use linear controller for this model. This paper descrisbes dynamic analysis and linear controller design for unicycle. PID controller is design for roll and pitch axis. The calibration of control parameters of each PID will be show and the respone will be included. Thence, LQR controller is designed for roll and pitch axis. The key of this controller is finding suitable values in matrices $\mathbf{Q}$ and $\mathbf{R}$. Thence, calibration of these values is included and shown to shown in simulation. Thence, linear controllers are proven to be effective for this model. Also, their calibration is shown to suit the theory [8-9].

2. Dynamic Operation:

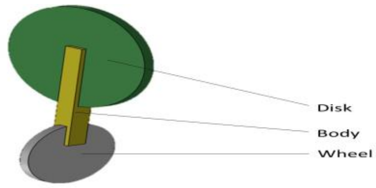

Fig. 1. Simplified model of the unicycle robot

In this section, we discuss the operation of unicycle robot. We will device this model to two independent body for pitch and roll axes of robot: one is inverted pendulum for pitch axis and reaction wheel balance inverted pendulum for roll axis. Dynamic models of the unicycle robot for the roll and pitch axes were derived using the Lagrange method. Fig. 1 shows the unicycle robot developed. Unicycle robot has 3 main parts: rotating disk, a robot body, and a rotating wheel, the mass are represented as m_d, m_b, and m_w.

2.1. Dynamic Model for Roll Axis

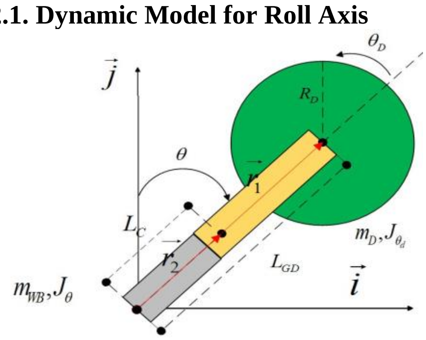

Fig. 2. Model of the unicycle robot for roll axis

Roll axis dynamic is calculated from model reaction wheel balance inverted pendulum consisting of two main parts: disk and body compound wheel which is considered a single body we call bottom body. Fig. 2 shows robot axes set to calculate dynamic roll. L_{GD} and L_C are denoted as distance from ground to center of the disk and distance from ground to center of gravity of bottom body, respectively. R_D and θ_D are denoted as radius and rotation angle of disk; θ is denoted as rotation angle in roll direction of robot. m_{WB}, m_B, m_D are mass bottom body, robot body and disk. Two position vectors $\vec{r_1}, \vec{r_2}$ are defined to caculate Lagrangian for robot. They represent vector from coordinate origin to center of disk and center of bottom body.

$$\vec{r_1} = L_C \sin(\theta)\vec{i} + L_C \cos(\theta)\vec{j} \tag{1}$$
$$\vec{r_2} = L_{GD} \sin(\theta)\vec{i} + L_{GD} \cos(\theta)\vec{j}$$

The robot's kinetic energy is calculated as follows:

$$K = \frac{1}{2} m_{WB}(\vec{v_1} \cdot \vec{v_1}) + \frac{1}{2} m_D(\vec{v_2} \cdot \vec{v_2}) + \frac{1}{2} J_\theta \dot{\theta}^2 \tag{2}$$
$$+\frac{1}{2} J_{\theta_d} (\dot{\theta} + \dot{\theta}_d)^2 \cos(\theta)\vec{j}$$

where $\vec{v_i} = d\vec{r_i} / dt$, J_D and J_θ are the inertia of disk and roll axis dynamic model.

The robot's position energy is calculated as follows:

$$U = m_{WB} g L_C \cos\theta + m_D g L_{GD} \cos(\theta) \tag{3}$$

where $g = 9.81(m/s^2)$

The Lagrangian L can be caculated:

$$L = K - U = \frac{1}{2}(\vec{v_1} \cdot \vec{v_1}) + \frac{1}{2} m_D(\vec{v_2} \cdot \vec{v_2}) + \tag{4}$$
$$+\frac{1}{2} J_\theta \dot{\theta} + \frac{1}{2} J_{\theta_d} (\dot{\theta} + \dot{\theta}_D)^2 \cos\theta\vec{j} +$$
$$-m_{GD} g L_C \cos\theta - m_D g L_{GD} \cos\theta$$

Using the Lagrange equation, we have:

$$\frac{d}{dt}\frac{\partial L}{\partial \dot{\mathbf{q}}} - \frac{\partial L}{\partial \mathbf{q}} = \tau_q \tag{5}$$

where $\mathbf{q} = \begin{bmatrix} \theta & \theta_D \end{bmatrix}^T$ and $\tau_q = \begin{bmatrix} \tau_\theta & \tau_{\theta_D} \end{bmatrix}^T$

The roll dynamics is caculated as follows:

$$\tau_\theta = (J_\theta + L^2{}_C m_{GD} + L^2{}_{GD} m_D)\ddot{\theta} \tag{6}$$
$$-g(L_C m_{GD} + L_{GD} m_D)\sin\theta$$
$$\tau_{\theta_D} = J_{\theta_d} (\ddot{\theta}_d + \ddot{\theta})$$

where τ_{θ_D} is rotational torque generated by motor of disk and rotational torque of roll axis single body, τ_θ has same value but opposite direction. So, we have $\tau_\theta = -\tau_{\theta_D}$.

Using upright condition, $\sin\theta \approx \theta$, (6) is presented as follow:

$$\tau_\theta = (J_\theta + L^2{}_C m_{GD} + L^2{}_{GD} m_D)\ddot{\theta} \tag{7}$$
$$-g(L_C m_{GD} + L_{GD} m_D)\theta$$
$$\tau_{\theta_D} = J_{\theta_d} (\ddot{\theta}_d + \ddot{\theta})$$

Torque of the pitch DC motor can be calculated by consider the motor dynamic with the robot dynamic [7], can be represented as:

$$T = n\frac{K_t}{R_m}(v + K_b(\dot{\theta} - \dot{\theta}_d)) + f_m(\dot{\theta} - \dot{\theta}_d) \tag{8}$$

where v_R is voltage of roll DC motor, $\dot{\theta} - \dot{\theta}_d$ is offset of the angular velocity of pitch axis dynamic model and the angular velocity of pitch DC motor. K_t, R_m, f_m, K_b are represented motor torque constant, motor resistance, motor friction coefficient and back e.m.f constant of motor.

With the equation (8), the external torque required for the roll DC motor and torque of the roll axis dynamic model can be obtained as:

$$\tau_{\theta_d} = -\alpha v_R - \beta(\dot{\theta} - \dot{\theta}_d);\ \tau_\theta = \alpha v_R + \beta(\dot{\theta} - \dot{\theta}_d) \tag{9}$$

with $\alpha = nKt / R_m, \beta = \alpha + f_m$.

with the result of (9), the eqution (7) can be obtained as:

$$\alpha v_R = (J_b + L^2{}_C m_{WB} + L^2{}_{GD} m_D)\ddot{\theta} \tag{10}$$
$$-g(L_C m_{WB} + L_{GD} m_D)\theta - \beta(\dot{\theta} - \dot{\theta}_D)$$
$$-\alpha v_R = J_d(\ddot{\theta}_D + \ddot{\theta}) + \beta(\dot{\theta} - \dot{\theta}_D)$$

2.2. Dynamic Model for Pitch Axis

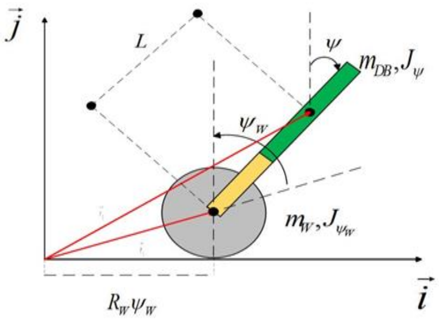

Fig. 3. Model of the unicycle robot for pitch axis

The pitch axis dynamic is calculated based on the model inverted pendulum consisting of two main parts: wheel and body compound disk which is considered a single body we call upper body. Fig. 3 demonstrates the robot axes set to calculate dynamic pitch. L are denoted as the distance from the center of the wheel to the center of the upper body. R_W is the radius of the wheel, while ψ_W and ψ are present rotational angle of the wheel and pitch axis dynamic model. m_W and m_{DB} are mass of the wheel and upper body. Two position vector $\vec{r_1}, \vec{r_2}$ defined to caculate the Lagrangian for the robot which are represent the vector from coordinate origin to the center of the wheel and the center of the upper body.

$$\vec{r_1} = R_W \psi_W \vec{i} + R_W \vec{j} \tag{11}$$

$$\vec{r_2} = (R_W \theta + L\sin\psi)\vec{i} + (R_W + L\cos\psi)\vec{j}$$

The robot's kinetic energy is calculated as follows:

$$K = \frac{1}{2} m_W (\vec{v_1} \cdot \vec{v_1}) + \frac{1}{2} m_{DB} (\vec{v_2} \cdot \vec{v_2}) + \tag{12}$$

$$+\frac{1}{2} J_{\psi_W} \dot{\psi}_W{}^2 + \frac{1}{2} J_\psi \dot{\psi}^2 + \frac{1}{2} n^2 J_m (\dot{\theta} - \dot{\psi})^2$$

where $\vec{v_i} = d\vec{r_i} / dt$, J_ψ, J_{ψ_W} and J_m are the inertias of the wheel, the pitch axis dynamic model , and the motor armature, respectively, and n is the gear ratio.

The robot's position energy is calculated as follows:

$$U = m_W g R_W + m_{DB} g (R_W + L\cos\psi) \tag{13}$$

Therefore, the Lagrangian L can be found as:

$$L = K - U = \tag{14}$$

$$\frac{1}{2} m_W (\vec{v_1} \cdot \vec{v_1}) + \frac{1}{2} m_{DB} (\vec{v_2} \cdot \vec{v_2}) +$$

$$+\frac{1}{2} J_{\psi_W} \dot{\psi}_W{}^2 + \frac{1}{2} J_\psi \dot{\psi}^2$$

$$= \frac{1}{2} n^2 J_m (\dot{\psi}_W - \dot{\psi})^2 - m_W g R_W +$$

$$- m_{DB} g (R_W + L\cos\psi)$$

Using the Lagrange equation, we have:

$$\tau_{\psi_W} = A_1 \ddot{\psi}_W + A_2 \ddot{\psi} + L m_{DB} R_W \sin\psi \dot{\psi}^2 \tag{15}$$

$$\tau_\psi = B_1 \ddot{\psi}_W + B_2 \ddot{\psi} - g L m_{DB} \sin\psi$$

Where $A_1 = J_{\psi_W} + J_m n^2 + (m_W + m_{DB}) R^2{}_W$;

$A_2 = L m_{DB} R_W \cos\psi - J_m n^2$;

$B_1 = L m_{DB} R_W \cos\psi - J_m n^2$;

$B_2 = J_\psi + L^2 m_{DB} + J_m n^2$; τ_{ψ_W} is the rotational torque generated by motor of wheel and τ_ψ is the rotational torque of the pitch axis dynamic model, has the same value but opposite direction so we have $\tau_{\psi_W} = \tau_\psi$.

Using upright condition, $\sin\psi \approx \psi$ and $\dot{\psi}^2 = 0$, we represent (15) as follow:

$$\tau_{\psi_W} = \left[J_{\psi_W} + J_m n^2 + (m_W + m_{BD}) R^2{}_W \right] \ddot{\psi}_W \tag{16}$$

$$+\left[L m_{DB} R_W - J_m n^2 \right] \ddot{\psi}$$

$$\tau_\psi = \left[L m_{DB} R_W - J_m n^2 \right] \ddot{\psi}_W - g l m_{DB} \psi$$

$$+\left[J_\psi + L^2 m_{DB} + J_m n^2 \right] \ddot{\psi}$$

Torque of the pitch DC motor can be calculated by consider the motor dynamic with the robot dynamics [7], can be represented as:

$$T = n \frac{K_t}{R_m} (v_P + K_b (\dot{\psi} - \dot{\psi}_W)) + f_m (\dot{\psi} - \dot{\psi}_W) \tag{17}$$

where v_P is voltage of pitch DC motor, $\dot{\psi} - \dot{\psi}_W$ is offset of the angular velocity of pitch axis dynamic model and the angular velocity of pitch DC motor. K_t, R_m, f_m, K_b are motor torque constant, motor resistance, motor friction coefficient and back e.m.f constant of motor.

From (17), external torque required for pitch DC motor and torque of pitch axis is obtained as:

$$\tau_{\psi_W} = -\alpha v_P - \beta (\dot{\psi} - \dot{\psi}_W) \tag{18}$$

$$\tau_\psi = \alpha v_P + \beta (\dot{\psi} - \dot{\psi}_W)$$

with $\alpha = nKt / R_m, \beta = \alpha + f_m$.

with the result of (18), the equation (16) can be obtained as:

$$\alpha v_P = \left(J_{\psi_W} + J_m n^2 + (m_W + m_{DB}) R^2{}_W \right) \ddot{\psi}_W \tag{19}$$

$$+\left(L m_{DB} R_W - J_m n^2 \right) \ddot{\psi} + \beta \dot{\psi}_W - \beta \dot{\psi}$$

$$-\alpha v_P = (L m_{DB} R_W - J_m n^2) \ddot{\psi}_W - \beta \dot{\psi}_W + \beta \dot{\psi}$$

$$- g L m_{DB} \psi + \left(J_\psi + L^2 m_{DB} + J_m n^2 \right) \ddot{\psi}$$

3. PID Controller

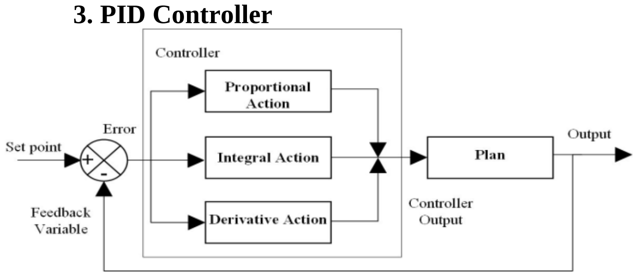

Fig. 4. PID Controller

Ifluence of PID parameters is shown in Tab. 1.

Tab. 1. Influence of PID parameters to response of system

Input response	Rise time	Overshoot	Transient	Setting error
K_P	Decrease	Increase	Small change	Decrease
K_D	Decrease	Increase	Increase	Eliminate
K_I	Small change	Decrease	Decrease	Small change

3.1. Simulation

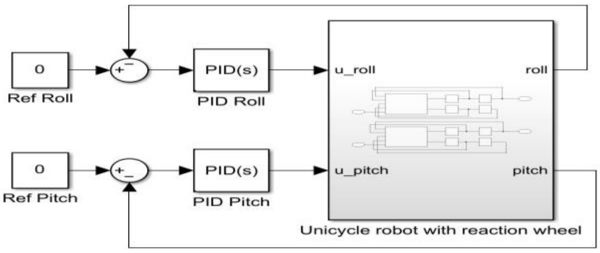

Fig. 5. Schematic of simulation of unicycle using PID control

3.2. Simulation Diagram

3.2.1 Standard PID

Select a set of PID parameters to control the system stably:

- Stable PID value of Roll axis

K_P=120; K_I=400; K_d=10 (20)

- Stable PID value of Pitch axis

K_P=300; K_I=700; K_d=30 (21)

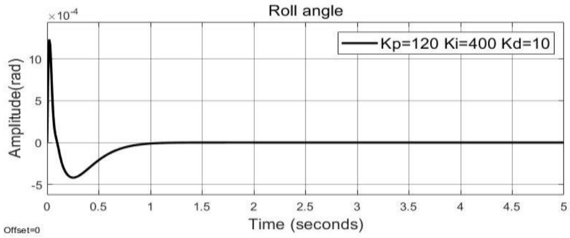

Fig. 6. Result of standard PID value Roll axis

Comment: We see that the output response has no overshoot phenomenon, the time for the system to balance at zero position is 1s and the setting error is 0.

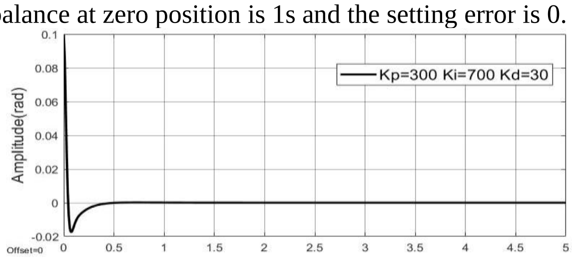

Fig. 7. Result of standard PID value Pitch axis

Comment: We see that the output response has no overshoot phenomenon, the time for the system to balance at zero position is 0.5s and the setting error is 0.

3.2.2. Change K_P Value

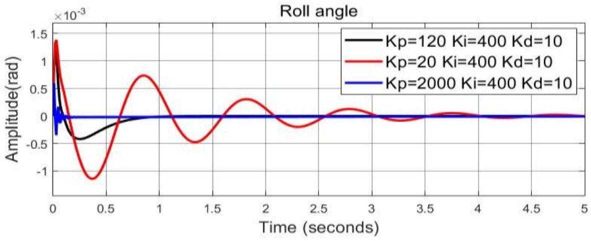

Fig. 8. Result of change in K_P value Roll axis

- Increase in K_P value Roll axis K_P =2000

Comment: We see that the output appears to fluctuate from [-0.3;0.6] (milirad) and the robot responds to the equilibrium position faster at t=0.2s. So we can understand that when increasing K_P, the motor will have to operate very quickly, easily causing motor damage.

- Decrease in K_P value Roll axis K_P =20

Comment: We see that the output appears to fluctuate from [-1.1;1.4] (milirad) and gradually decrease until the robot responds to the equilibrium position at t=6s.

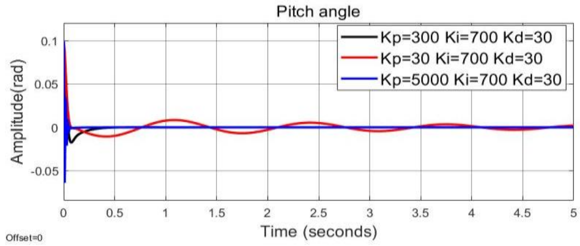

Fig. 9: Result of change K_P in value Pitch axis

- Increase in K_P value Pitch axis K_P =5000

Comment: We see that the output appears to fluctuate from [-0.06;0.1] (rad) and the robot responds to the equilibrium position faster at t=0.2s. So we can understand that when increasing K_P, the motor will have to operate very quickly, easily causing motor damage.

- Decrease in K_P value Pitch axis K_P =30

Comment: We see that the output overshoots up to 0.1 (rad) at t=0.1s, then fluctuates in the range [-0.01;0.01] and gradually decreases until the robot stabilizes in a balanced position at t=12s.

3.2.3. Change K_I Value

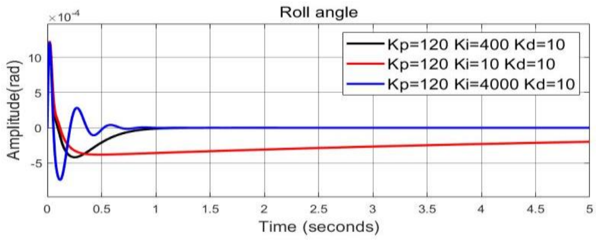

Fig. 10. Result of change K_I value Roll axis

- Increase in K_I value Roll axis K_I =4000

Comment: We see that the output overshoots up to 1 millirad at t=0.1s then oscillates in the range [-0.7;0.3] (milirad) and gradually decreases until the robot stabilizes in a balanced position at t= 1s.

- Decrease in K_I value Roll axis K_I =10

Comment: Output overshoots up to 1.5 (millirad) at t=0.1s, then drops to -0.4 (millirad) at t=0.2s and gradually approaches equilibrium position after more than 20s.

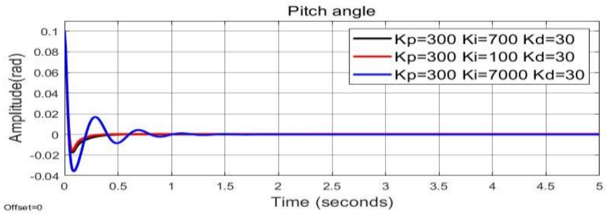

Fig. 11. Result of change K_I value Pitch axis

- Increase in K_I value Pitch axis K_I=7000

Comment: Output appears to fluctuate in [-0.03;0.02] (rad) and gradually returns to equilibrium position at t=1.8s.

- Decrease in K_I value Pitch axis K_I=10

Comment: Output has no overshoot, fluctuates slightly and responds quickly at t=0.2s and at same time, there is a setting error exl=0.001 (rad).

3.2.4. Change K_D Value

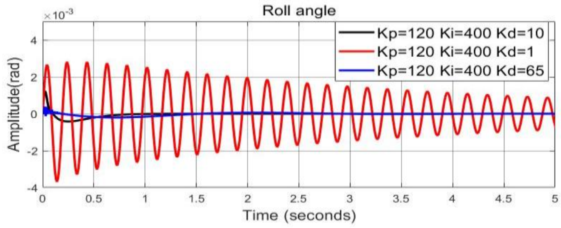

Fig. 12. Result of change K_D value Roll axis

- Increase in K_D value Roll axis K_D=65

Comment: Output appears to fluctuate slightly around equilibrium position and gradually stabilizes to 0 at t=3s

- Decrease in K_D value Roll axis K_D=1

Comment: Output appears to fluctuate symmetrically in [-3.8;2.8] (milirad) and tends to gradually decrease and stabilize at equilibrium position at t=18s.

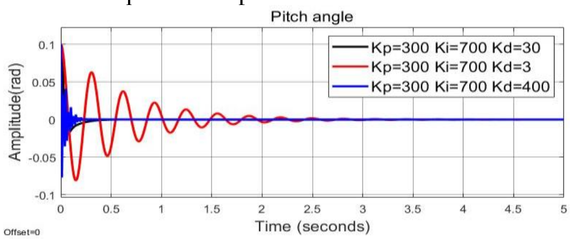

Fig. 13. Result of change K_D value Pitch axis

- Increase in K_D value Pitch axis K_D=400

Comment: Output appears to fluctuate symmetrically in [-3.8-2.8] (milirad) and tends to gradually decrease and stabilize at equilibrium position at t=18s.

- Decrease in K_D value Pitch axis K_D=3

Comment: Output appears to fluctuate symmetrically in [-3.8-2.8] (milirad) and tends to gradually decrease and stabilize at equilibrium position at t=18s.

4. LQR Controller

4.1. LQR Controller for Roll Axis

With equation (10) we obtain the simultaneous equation describe the system:

$$\begin{cases} \dot{x}_1 = x_2 \\ \dot{x}_2 = f_2(x_1, x_2, x_4, x_5, u) \\ \dot{x}_4 = x_5 \\ \dot{x}_5 = f_5(x_1, x_2, x_4, x_5, u) \end{cases} \quad (22)$$

where

$$x = \begin{bmatrix} x_1 & x_2 & x_4 & x_5 \end{bmatrix}^T = \begin{bmatrix} \theta & \dot{\theta} & \theta_D & \dot{\theta}_D \end{bmatrix}^T \quad (23)$$

We choose the work position:

$$x_0 = \begin{bmatrix} 0 & 0 & 0 & 0 \end{bmatrix}^T ;\ u_0 = \begin{bmatrix} 0 \end{bmatrix}^T \quad (24)$$

So that we can linear the simultaneous equation (22) as:

$$\dot{x} = \mathbf{A}x + \mathbf{B}u ;\ y = \mathbf{C}x + \mathbf{D} \quad (25)$$

$$u = \begin{bmatrix} v_R \end{bmatrix} \quad (26)$$

$$\mathbf{A} = \begin{bmatrix} 0 & 1 & 0 & 0 \\ \left.\frac{\partial f_2}{\partial x_1}\right|_{\substack{x=x_0 \\ u=u_0}} & \left.\frac{\partial f_2}{\partial x_2}\right|_{\substack{x=x_0 \\ u=u_0}} & \left.\frac{\partial f_2}{\partial x_4}\right|_{\substack{x=x_0 \\ u=u_0}} & \left.\frac{\partial f_2}{\partial x_5}\right|_{\substack{x=x_0 \\ u=u_0}} \\ 0 & 0 & 0 & 1 \\ \left.\frac{\partial f_4}{\partial x_1}\right|_{\substack{x=x_0 \\ u=u_0}} & \left.\frac{\partial f_4}{\partial x_2}\right|_{\substack{x=x_0 \\ u=u_0}} & \left.\frac{\partial f_4}{\partial x_4}\right|_{\substack{x=x_0 \\ u=u_0}} & \left.\frac{\partial f_4}{\partial x_5}\right|_{\substack{x=x_0 \\ u=u_0}} \end{bmatrix} \quad (27)$$

$$\mathbf{B} = \begin{bmatrix} 0 & \left.\frac{\partial f_2}{\partial v_R}\right|_{\substack{x=x_0 \\ u=u_0}} & 0 & \left.\frac{\partial f_4}{\partial v_R}\right|_{\substack{x=x_0 \\ u=u_0}} \end{bmatrix}^T \quad (28)$$

The matrix $\mathbf{Q}, \mathbf{R}$ we can obtain as:

$$\mathbf{Q} = \begin{bmatrix} Q_1 & 0 & 0 & 0 \\ 0 & Q_2 & 0 & 0 \\ 0 & 0 & Q_3 & 0 \\ 0 & 0 & 0 & Q_4 \end{bmatrix}; \quad \mathbf{R} = [R_1] \quad (29)$$

The coefficient Q_1, Q_2, Q_3, Q_4 show priority of variable status x_1, x_2, x_4, x_5. If increasing one on four coefficient, variable corresponding is better responded than others, maybe that change can make system balance but it can be make our robot imbalance. So that we need choose matrix $\mathbf{Q}$ carefully. Matrix $\mathbf{R}$ shows priority of input v_R. The matrices $\mathbf{Q}, \mathbf{R}$ were selected as follow:

$$\mathbf{Q} = \begin{bmatrix} 350 & 0 & 0 & 0 \\ 0 & 10 & 0 & 0 \\ 0 & 0 & 100 & 0 \\ 0 & 0 & 0 & 10 \end{bmatrix}; \quad \mathbf{R} = [1] \quad (30)$$

The optimal gain can be solved by LQR toolbox in MATLAB [8], [9] as:

$$K = [\,-34.9638 \quad -4.0849 \quad -10.0000 \quad -8.1591\,] \tag{31}$$

Control input is given as:

$$v_R = -Kx \tag{32}$$

where $x = [x_1 \quad x_2 \quad x_4 \quad x_5]^T = [\theta \quad \dot{\theta} \quad \theta_D \quad \dot{\theta}_D]^T$;

$e_\theta = \theta - \theta_{ref}$; $e_{\theta_D} = \theta_D - \theta_{Dref}$

4.2. LQR Controller for Pitch Axis

With (19), we obtain the simultaneous equation describe the system:

$$\begin{cases} \dot{x}_7 = x_8 \\ \dot{x}_8 = f_6(x_7, x_8, x_{10}, x_{11}, u) \\ \dot{x}_{10} = x_{11} \\ \dot{x}_{11} = f_8(x_7, x_8, x_{10}, x_{11}, u) \end{cases} \tag{33}$$

with

$$x = [x_7 \quad x_8 \quad x_{10} \quad x_{11}]^T = [\psi_W \quad \dot{\psi}_W \quad \psi \quad \dot{\psi}]^T \tag{34}$$

We choose the work position:

$$x_0 = [0 \quad 0 \quad 0 \quad 0]^T; u_0 = [0]^T \tag{35}$$

So that we can linear the simultaneous equation (33) as:

$$\dot{x} = \mathbf{A}x + \mathbf{B}u; y = \mathbf{C}x + \mathbf{D} \tag{36}$$

where

$$u = [v_P] \tag{37}$$

$$\mathbf{A} = \begin{bmatrix} 0 & 1 & 0 & 0 \\ \left.\frac{\partial f_6}{\partial x_7}\right|_{\substack{x=x_0\\u=u_0}} & \left.\frac{\partial f_6}{\partial x_8}\right|_{\substack{x=x_0\\u=u_0}} & \left.\frac{\partial f_6}{\partial x_{10}}\right|_{\substack{x=x_0\\u=u_0}} & \left.\frac{\partial f_6}{\partial x_{11}}\right|_{\substack{x=x_0\\u=u_0}} \\ 0 & 0 & 0 & 1 \\ \left.\frac{\partial f_8}{\partial x_7}\right|_{\substack{x=x_0\\u=u_0}} & \left.\frac{\partial f_8}{\partial x_8}\right|_{\substack{x=x_0\\u=u_0}} & \left.\frac{\partial f_8}{\partial x_{10}}\right|_{\substack{x=x_0\\u=u_0}} & \left.\frac{\partial f_8}{\partial x_{11}}\right|_{\substack{x=x_0\\u=u_0}} \end{bmatrix} \tag{38}$$

$$\mathbf{B} = \begin{bmatrix} 0 & \left.\frac{\partial f_6}{\partial v_P}\right|_{\substack{x=x_0\\u=u_0}} & 0 & \left.\frac{\partial f_8}{\partial v_P}\right|_{\substack{x=x_0\\u=u_0}} \end{bmatrix}^T \tag{39}$$

We can obtain as:

$$\mathbf{Q} = \begin{bmatrix} Q_5 & 0 & 0 & 0 \\ 0 & Q_6 & 0 & 0 \\ 0 & 0 & Q_7 & 0 \\ 0 & 0 & 0 & Q_8 \end{bmatrix}; \quad \mathbf{R} = [R_2] \tag{40}$$

The matrix $\mathbf{Q}, \mathbf{R}$ were selected as follow:

$$\mathbf{Q} = \begin{bmatrix} 350 & 0 & 0 & 0 \\ 0 & 10 & 0 & 0 \\ 0 & 0 & 100 & 0 \\ 0 & 0 & 0 & 10 \end{bmatrix}; \quad \mathbf{R} = [1] \tag{41}$$

Then, it yields

$$K = [48.1396 \quad 10.3124 \quad 10.0000 \quad 10.3962] \tag{42}$$

Control input is given as:

$$v_P = -Kx \tag{43}$$

where $x = [x_7 \quad x_8 \quad x_{10} \quad x_{11}]^T = [\psi_W \quad \dot{\psi}_W \quad \psi \quad \dot{\psi}]^T$;

$e_{\psi_W} = \psi_W - \psi_{Wref}$; $e_\psi = \psi - \psi_{ref}$

4.3. Simulation

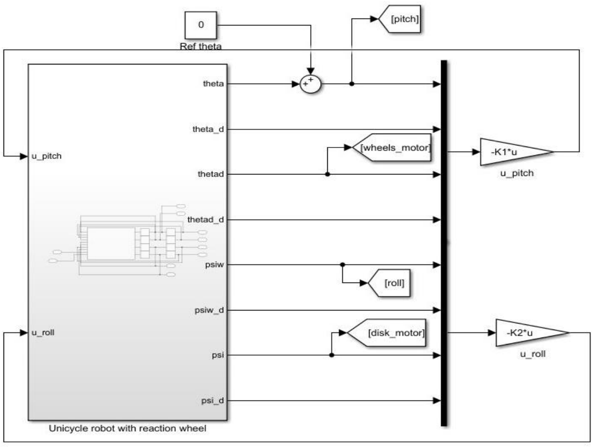

Fig. 14. Simulation of unicycle using a LQR controller

4.4. Simulation Diagram

4.4.1. Standard LQR

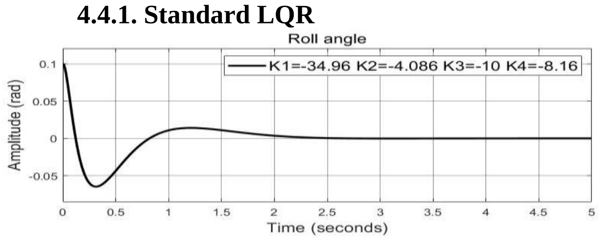

Fig. 15. Stable LQR value of Roll axis

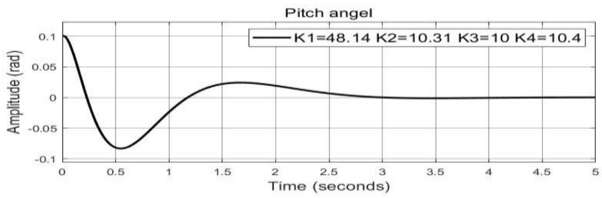

Fig. 16. Stable LQR value for Pitch axis

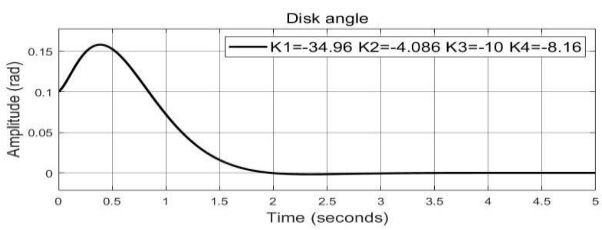

Fig. 17. Output result of the disk motor

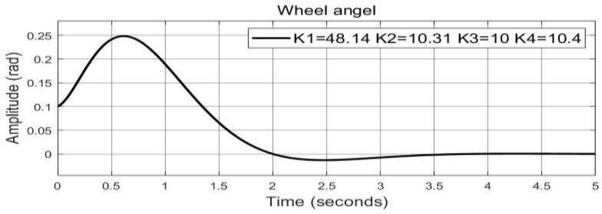

Fig. 18. Output result of wheel motor

Comment: With the standard value, roll angle starts from 0.06 rad and decreases to -0.06 rad after 0.5s. Then, it gradually increases and stabilizes at 0 position at t=2.5s. Pitch angle fluctuates from 0.1 to -0.075 in 0.75s and reaches 0 at t=4s.

4.4.2. Change Q_1 and Q_5 Values

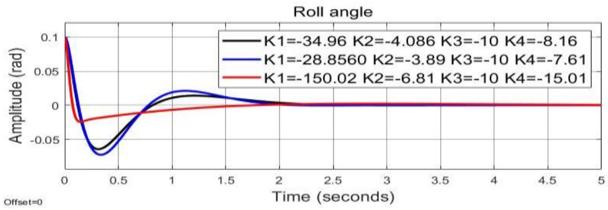

Fig. 19. Result change Q_1 value for Roll axis

- Increase Q_1:

$$\mathbf{Q} = \begin{bmatrix} 20000 & 0 & 0 & 0 \\ 0 & 10 & 0 & 0 \\ 0 & 0 & 100 & 0 \\ 0 & 0 & 0 & 10 \end{bmatrix}$$

$$\rightarrow K = [\text{-150.0257} \quad \text{-6.8157} \quad \text{-10.0000} \quad \text{-15.0139}]$$

- Decrease Q_1:

$$\mathbf{Q} = \begin{bmatrix} 50 & 0 & 0 & 0 \\ 0 & 10 & 0 & 0 \\ 0 & 0 & 100 & 0 \\ 0 & 0 & 0 & 10 \end{bmatrix}$$

$$\rightarrow K = [\text{-28.8560} \quad \text{-3.8918} \quad \text{-10.0000} \quad \text{-7.6135}]$$

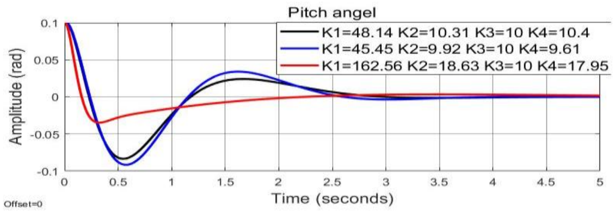

Fig. 20. Result change Q_5 value for Pitch axis

- Increase Q_5:

$$\mathbf{Q} = \begin{bmatrix} 600 & 0 & 0 & 0 \\ 0 & 10 & 0 & 0 \\ 0 & 0 & 100 & 0 \\ 0 & 0 & 0 & 10 \end{bmatrix}$$

$$\rightarrow K = [52.2130 \quad 10.7153 \quad 10.0000 \quad 10.7610]$$

- Decrease Q_5:

$$\mathbf{Q} = \begin{bmatrix} 50 & 0 & 0 & 0 \\ 0 & 10 & 0 & 0 \\ 0 & 0 & 100 & 0 \\ 0 & 0 & 0 & 10 \end{bmatrix}$$

$$\rightarrow K = [42.3111 \quad 9.7083 \quad 10.0000 \quad 9.8496]$$

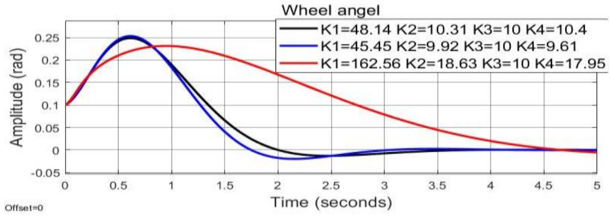

Fig. 21. Output result of the wheel motor

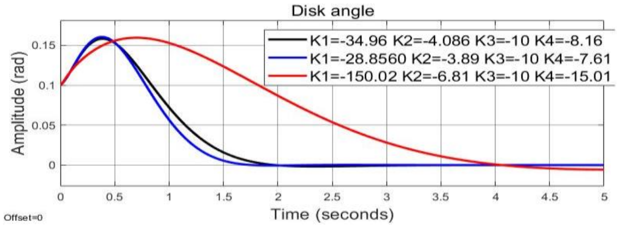

Fig. 22. Output result of the disk motor

Comment:

- When increasing Q_1, roll angle has an overshoot of 0.1(rad) at t=0.1s. Then, it decreases to -0.02 rad and gradually increases slightly until it meets equilibrium position at t=5s (slower response time). When decreasing Q_1, roll angle reaches -0.07 rad at t=0.5s and tends to increase rapidly to 0.02 rad in next 0.5s. Then, it gradually decreases to 0 at t=2s (faster response time).

- When increasing Q_5, pitch angle has overshoot of 0.1 rad at initial time. Then, it decreases to -0.03rad and gradually increases slightly until it meets equilibrium position at t=8s (slower response time). When decreasing Q_5, pitch angle reaches -0.09 rad at t=0.5s and tends to increase rapidly to 0.03 rad in next 1s. Then, it gradually decreases to 0 at t=4s (faster response time).

- When the pitch angle changes, if increasing Q_5, pitch angle skyrockets to 0.4rad (more than standard value) and the response time is quite long, taking about t=14s to return to 0 position. If decreasing Q_5 pitch angle responds to equilibrium position faster than 0.5s and signal sticks closed to the standard value.

- When roll angle changes, if increasing Q_1, roll angle has a long response time, taking about 8s to return to 0 position (2 times longer than standard value). If decreasing Q_1, roll angle responds. Position is balanced and signal is closed to standard value.

4.4.3. Change Q_2 and Q_6 Values

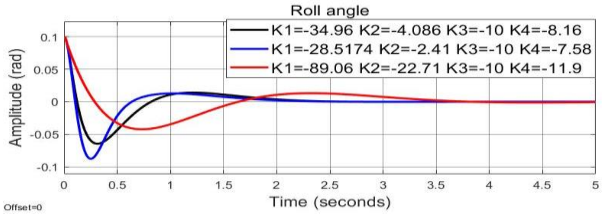

Fig. 23. Result change Q_2 value for Roll axis

- Increase Q_2:

$$\mathbf{Q} = \begin{bmatrix} 350 & 0 & 0 & 0 \\ 0 & 500 & 0 & 0 \\ 0 & 0 & 100 & 0 \\ 0 & 0 & 0 & 10 \end{bmatrix}$$

$$\rightarrow K = [\text{-89.0608} \;\; \text{-22.7104} \;\; \text{-10.0000} \;\; \text{-11.9059}]$$

- Decrease Q_2:

$$\mathbf{Q} = \begin{bmatrix} 350 & 0 & 0 & 0 \\ 0 & 0.0001 & 0 & 0 \\ 0 & 0 & 100 & 0 \\ 0 & 0 & 0 & 10 \end{bmatrix}$$

$$\rightarrow K = [\text{-28.5174} \;\; \text{-2.4166} \;\; \text{-10.0000} \;\; \text{-7.5820}]$$

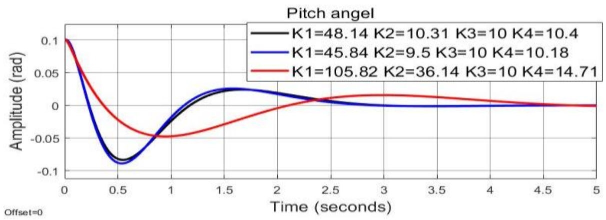

Fig. 24. Result change Q_6 value for Pitch axis

- Increase Q_6:

$$\mathbf{Q} = \begin{bmatrix} 350 & 0 & 0 & 0 \\ 0 & 1000 & 0 & 0 \\ 0 & 0 & 100 & 0 \\ 0 & 0 & 0 & 10 \end{bmatrix} \rightarrow K = [105.8238 \;\; 36.1443 \;\; 10.0000 \;\; 14.7162]$$

- Decrease Q_6:

$$\mathbf{Q} = \begin{bmatrix} 350 & 0 & 0 & 0 \\ 0 & 0.0001 & 0 & 0 \\ 0 & 0 & 100 & 0 \\ 0 & 0 & 0 & 10 \end{bmatrix} \rightarrow K = [45.8420 \;\; 9.4896 \;\; 10.0000 \;\; 10.1844]$$

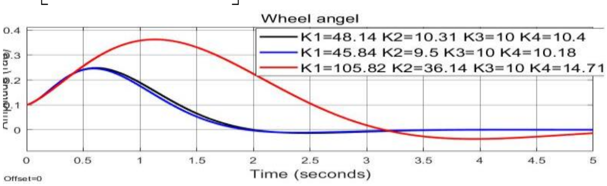

Fig. 25. Output result of the wheel motor

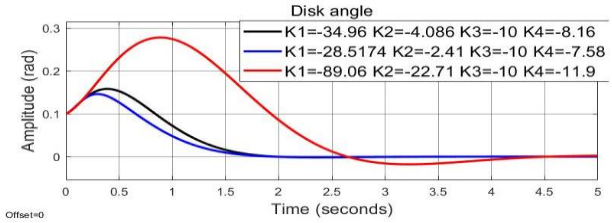

Fig. 26. Output result of the disk motor

Comment: We see that

- When increasing Q_2, roll angle has an overshoot of 0.1 rad at initial time. Then, it decreases to -0.04(rad) and gradually increases slightly until it meets the equilibrium position at t=6s (slower response time). When decreasing Q_2, roll angle reaches -0.08 rad at t=0.5s (more than the standard value) and tends to increase rapidly to 0.015 in the next 1s, then gradually decreases to 0 at t=2.5s (response time is almost equal to the standard value).

- When increasing Q_6, pitch angle has an overshoot of 0.1 rad at initial time. Then, it decreases to -0.045 rad and gradually increases slightly until it meets equilibrium position at t=7s (response time is much slower). double compared to the standard value). When decreasing Q_6, pitch angle reaches -0.08 rad at t=0.5s and tends to increase rapidly to 0.03 rad in the next 1s, then gradually decreases to 0 at t=3s (response time similar to standard value).

- When roll angle changes, if increasing Q_2, roll angle overshoots to 0.275 rad at t=1s and has a fairly long response time, taking about 6s to return to 0 position (3 times longer than the standard value). Meanwhile, if Q_2 is reduced, roll angle has less overshoot, response time and the tracking signal are closer to standard value.

- When pitch angle changes, if increasing Q_6, pitch angle skyrockets to 0.36 rad (more than standard value) and response time is quite long, taking 8s to return to 0 position. If decreasing Q_6, pitch angle meets equilibrium point and signal is closed to standard value.

4.4.4. Change Q_3 and Q_7 Values

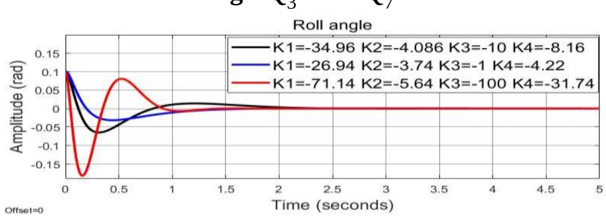

Fig. 27. Result change Q_3 value for Roll axis

- Increase Q_3:

$$\mathbf{Q}=\begin{bmatrix}350&0&0&0\\0&10&0&0\\0&0&10000&0\\0&0&0&10\end{bmatrix}\rightarrow K=\left[\text{-71.1442}\ \ \text{-5.6425}\ \ \text{-100.0000}\ \ \text{-31.7406}\right]$$

- Decrease Q_3:

$$\mathbf{Q}=\begin{bmatrix}350&0&0&0\\0&10&0&0\\0&0&1&0\\0&0&0&10\end{bmatrix}\rightarrow K=\left[\text{-26.9381}\ \ \text{-3.7431}\ \ \text{-1.0000}\ \ \text{-4.2220}\right]$$

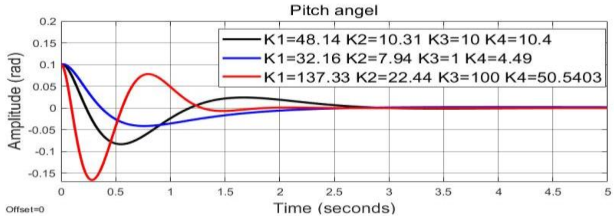

Fig. 28. Result Q_7 change value for Pitch axis

- Increase Q_7:

$$\mathbf{Q}=\begin{bmatrix}350&0&0&0\\0&10&0&0\\0&0&10000&0\\0&0&0&10\end{bmatrix}\rightarrow K=\left[137.3350\ \ 22.4459\ \ 100.0000\ \ 50.5403\right]$$

- Decrease Q_7:

$$\mathbf{Q}=\begin{bmatrix}350&0&0&0\\0&10&0&0\\0&0&1&0\\0&0&0&10\end{bmatrix}\rightarrow K=\left[32.1629\ \ 7.9376\ \ 1.0000\ \ 4.4936\right]$$

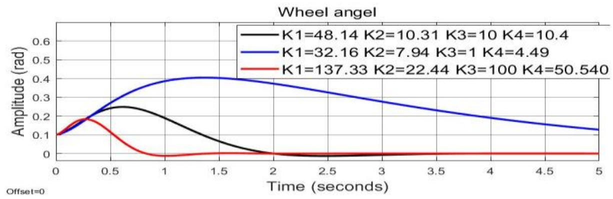

Fig. 29. Output result of the wheel motor

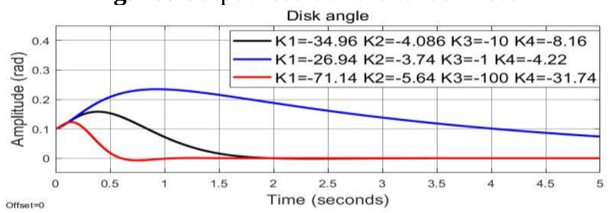

Fig. 30. Output result of the disk motor

We see that:

- When increasing Q_3, troll angle has an overshoot of 0.1 rad at initial time, then, it decreases to -0.175 rad and gradually increases until it meets equilibrium position at t=1.75s (faster response time). When decreasing Q_3, roll angle reaches -0.03 rad at t=0.5s (less than standard value) and tends to 0 at t=2.15s (response time is almost equal to the standard value).

- When increasing Q_7, pitch angle has overshoot of 0.1 rad at initial time. Then, it decreases to -0.2 rad and oscillation gradually decreases until it meets equilibrium position at t=2s (response time). It is twice as fast as the standard value. When decreasing Q_7, pitch angle reaches -0.08 rad at t=0.5s and tends to increase rapidly to 0.03 in the next 1s. Then, it gradually decreases to 0 at t=4s (response time is similarly to value standard).

- When roll angle changes, if reducing Q_3, roll angle overshoots to 0.225 rad at t=1s, which has a fairly long response time, taking about 18s to return to 0 position (9 times longer than standard value). Meanwhile, if Q_3 is increased, roll angle has less overshoot, response time for equilibrium position and tracking signal are twice as good as the standard value.

- When pitch angle changes, if reducing Q_7, pitch angle increases to 0.41 rad (nearly twice as much as the standard value) and response time is quite long, taking about 14s to return to the 0 position. If increasing Q_7, pitch angle meets balanced position and signal tracks 2.5 times better than standard value.

4.4.5. Change Q_4 and Q_8 Values

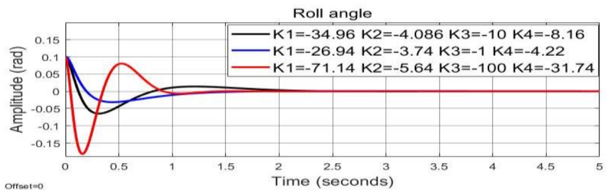

Fig. 31. Result change Q_4 value for Roll axis

- Increase Q_4:

$$\mathbf{Q}=\begin{bmatrix}350&0&0&0\\0&10&0&0\\0&0&100&0\\0&0&0&1000\end{bmatrix}\rightarrow K=\left[\text{-80.8838}\ \ \text{-6.0648}\ \ \text{-10.0000}\ \ \text{-33.7887}\right]$$

- Decrease Q_4:

$$\mathbf{Q}=\begin{bmatrix}350&0&0&0\\0&10&0&0\\0&0&100&0\\0&0&0&0.01\end{bmatrix}\rightarrow K=\left[\text{-33.1092}\ \ \text{-4.0057}\ \ \text{-10.0000}\ \ \text{-7.3014}\right]$$

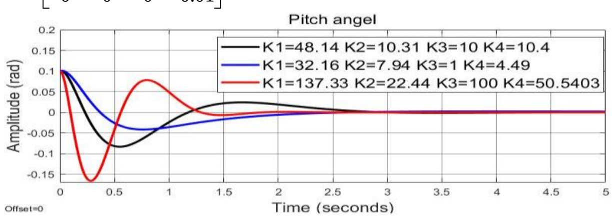

Fig. 32. Result change Q_8 value for Pitch axis

- Increase Q_8:

$$\mathbf{Q}=\begin{bmatrix}350 & 0 & 0 & 0\\ 0 & 10 & 0 & 0\\ 0 & 0 & 100 & 0\\ 0 & 0 & 0 & 1000\end{bmatrix}\rightarrow K=\begin{bmatrix}128.0682 & 21.2202 & 10.0000 & 35.5894\end{bmatrix}$$

Decrease Q_8 **:**

$$\mathbf{Q}=\begin{bmatrix}350 & 0 & 0 & 0\\ 0 & 10 & 0 & 0\\ 0 & 0 & 100 & 0\\ 0 & 0 & 0 & 0.01\end{bmatrix}\rightarrow K=\begin{bmatrix}45.45 & 9.9228 & 10.0000 & 9.6172\end{bmatrix}$$

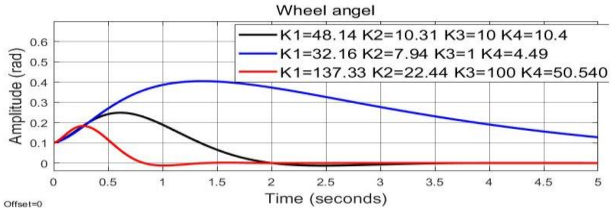

Fig. 33. Output result for the wheel motor

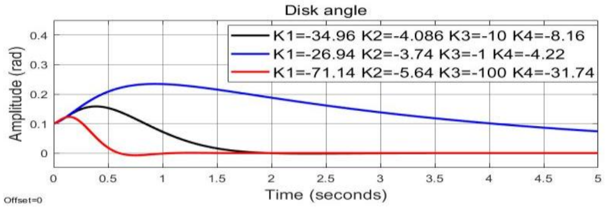

Fig. 34. Output result for the disk motor

We see that

- When increasing Q_4, roll angle fluctuates in [-0.065; 1] in 0.5s and meets equilibrium position at t=0.75s (response time is nearly twice as fast as standard value). When decreasing Q_4, roll angle follows signal and tends to 0, almost equal to standard value.

- When increasing Q_8, pitch angle has an overshoot of 0.1rad at initial time, then decreases to -0.6 rad in 0.5s and gradually increases until it meets equilibrium position at t=1s (fast response time, 4 times more than standard value). When decreasing Q_8, pitch angle fluctuates from [-0.7;0.7] for a period of 0.5s and then returns to 0 at t=4s (response time is similarly to standard value).

- When roll angle changes, if decreasing Q_4, roll angle follows the signal and has a time to respond to equilibrium position almost equal to the standard value. If increasing Q_4, roll angle has less overshoot and time. Responds to equilibrium position are 12s later than standard value.

- When pitch angle changes, if increasing Q_8, pitch angle decreases overshoot and response time is quite long, taking about 16 s to reach 0 position. If decreasing Q_8, pitch angle meets balanced position and signal follows closely as equal to standard value.

5. Conclusions

From this paper, we present steps to obtain dynamic equations of a unicycle. Thence, PID and LQR controllers are present to balance it at equilibrium point. The success of our algorithm is proven well through simulation. Also, from simulation, adjustments of control parameters of these controllers are operarted. The results suit points in theory. Thence, from this study, effectiveness of linear controllers are confirm for this highly-nonliear model.

6. References

[1] Schoonwinkel A.: “Design and test of a computer stabilized unicycle”, Ph.D. dissertation, Stanford Univ., Stanford, CA, 1987.

[2]. Sheng Z., Yamafuji K.: “Postural stability of a human riding a unicycle and its emulation by a robot”, IEEE Trans. Robot. Autom., vol. 13, no. 5, pp. 709–720, 1997.

[3] Lee J.-H. et al: “Novel air blowing control for balancing a unicycle robot”, in Proc. IEEE/RSJ Int. Conf. Intell. Robots Syst., pp. 2529–2530, 2010.

[4] Lee J. et al: ”Decoupled Dynamic Control for Pitch and Roll Axes of the Unicycle Robot”, IEEE Transactions on Industrial Electronics, vol. 60, no. 9, 2013.

[5] Ik H.S., Lee J:. “Balancing and Velocity Control of a Unicycle Robot Based on the Dynamic Model62, pp. 405-413, 2015.”, IEEE Transactions on Industrial Electronics

[6] Shen J., Hong D.:”OmBURo: A Novel Unicycle Robot with Active Omnidirectional Wheel”, IEEE International Conference on Robotics and Automation (ICRA), *pp. 8237-8243, 2020.*

[7] NXTway-GS (self-balancing two-wheeled robot) controllerdesign,LEGOMindstorm,Enfield,CT,Tech.Rep [Online].Available:htp://www.mathworks.com/matlabcentral/fileexchange/19147.

[8]. Dorf R.C., Bishop R.H.: „Modern Control System, 10th Edition:Optimal Control System”, Upper Saddle River, NJ: Pearson, 2005.

[9]. Tanaka Y., Murakami T.: “A study on straight-line tracking and posturecontrol in electric bicycle”, IEEE Trans. Ind. Electron., vol. 56, no. 1, pp. 159–168, 2009.